Available online at www.sciencedirect.com
ScienceDirect
Solar Energy Materials & Solar Cells 92 (2008) 673–681
Solar Energy Materials and Solar Cells
www.elsevier.com/locate/solmat

Letter

# Design optimization of bifacial HIT solar cells on p-type silicon substrates by simulation

L. Zhao*, C.L. Zhou, H.L. Li, H.W. Diao, W.J. Wang

*Laboratory of Solar Cell Technology, Institute of Electrical Engineering, The Chinese Academy of Sciences, Beijing 100080, China*

Received 13 November 2007; received in revised form 25 January 2008; accepted 30 January 2008

**Abstract**

Heterojunction with intrinsic thin layer (HIT) solar cells fabricated on p-type silicon substrates usually demonstrate inferior performance than those formed on n-type substrates. The influence of various structure parameters on the performance of the c-Si(p)-based bifacial HIT solar cell, i.e., the TCO/a-Si:H(n)/a-Si:H(i)/c-Si(p)/a-Si:H(i)/a-Si:H($p^+$)/TCO solar cell, was investigated in detail by computer simulation using the AFORS-HET software. The work function of the transparent conductive oxide was found to be a key factor to affect the solar cell performance. Detailed influence mechanisms were analysed. Accordingly, the design optimization of the bifacial HIT solar cells on c-Si(p) substrates was provided.


*Keywords:* HIT; Transparent conductive oxide; Work function; Simulation

## 1. Introduction

Based on an n-type Czochralski silicon textured absorber, SANYO Ltd. has developed a silicon heterojunction solar cell called heterojunction with intrinsic thin layer (HIT) with an efficiency over 20% [1]. Fabrication of HIT involves depositing thin hydrogenated amorphous silicon (a-Si:H) layers on both sides of a high-quality crystalline silicon (c-Si) wafer by plasma-enhanced chemical vapour deposition. This process can realize excellent surface passivation and p–n junction formation simultaneously. The low processing temperature (<200 °C) prevents the bulk property degradation of the substrate that is usually observed in high-temperature processes. Further, compared with the conventional diffused solar cells, HIT solar cells have a better temperature coefficient and a higher open-circuit voltage ($V_{OC}$) [2–4]. For these reasons, HIT solar cells have been extensively investigated.

Although SANYO's original design used an n-type substrate as the absorber for the HIT solar cell, current researches concentrate on developing the HIT solar cell on a p-type substrate, because of its popularity in the photovoltaic industry [5–7]. However, inferior performance was observed for devices fabricated on c-Si(p) as compared with those on c-Si(n). This was once attributed to the poor back surface field (BSF) effect at the c-Si(p)/a-Si:H($p^+$) interface due to the large valence band offset there [8,9]. Recently, NREL obtained a decent HIT performance on c-Si(p) utilizing the a-Si:H($p^+$) BSF [10], which suggests that a further investigation is necessary to fully understand the factors that affect the performance of the c-Si(p)-based HIT solar cell, although such work has been carried out to some extent [11,12].

Owing to the large number of processing variables, such as the doping concentration of the amorphous emitter, the thickness of the intrinsic amorphous layer, the band alignment of amorphous/crystalline Si heterojunction, etc.; it is a formidable task to scrutinize the effect of each variable on the performance of the solar cell experimentally. Numerical simulation using AMPS or AFORS-HET software provides a convenient way to accurately evaluate the role of various parameters [12–14]. Here, the performance of the c-Si(p)-based bifacial HIT solar cell, i.e., the TCO/a-Si:H(n)/a-Si:H(i)/c-Si(p)/a-Si:H(i)/a-Si:H($p^+$)/TCO solar cell, was investigated by utilizing the AFORS-HET software as

*Corresponding author.
*E-mail address:* zhaolei@mail.iee.ac.cn (L. Zhao).

0927-0248/$ - see front matter © 2008 Elsevier B.V. All rights reserved.
doi:10.1016/j.solmat.2008.01.018

the numerical simulation tool. The influence of various parameters for the front and the back structures was studied particularly. It was found that the work function of the transparent conductive oxide ($W_{TCO}$) was a key factor to affect the solar cell performance. Detailed influence mechanisms were analysed. Accordingly, the design optimization of the bifacial HIT solar cells on c-Si(p) substrates was provided.

## 2. Simulation

AFORS-HET solves the one-dimensional semiconductor equations based on Shockley–Read–Hall recombination statistics [11,12]. Here, the gap state densities of all kinds of the a-Si:H layers and the c-Si(p) base were set as the default values in AFORS-HET. The corresponding distributions were depicted in Fig. 1. The interface state density of the a-Si:H/c-Si interface was fixed as $1.2\times10^{11}\,cm^{-2}\,eV^{-1}$, which can be obtained by the conventional HF treatment (HF-dip) [15]. The surface recombination velocities of both electrons and holes were set as $1.0\times10^{7}\,cm\,s^{-1}$. The solar AM1.5 radiation was adopted as the illuminating source with a power density of $100\,mW\,cm^{-2}$. The light reflection of the front and the back contacts was set to be 0.1 and 1, respectively. The other simulating parameters were given the initial values as shown in Table 1. During the simulations, all the parameters were adopted as the above setting values except for the specific declared ones.

## 3. Results and discussion

### 3.1. Optimization of the front structure

#### 3.1.1. Influence of the doping concentration of the a-Si:H(n) emitter ($N_e$)

Fig. 2 gives the performance of the TCO/a-Si:H(n)/c-Si(p) solar cell as a function of $N_e$ with the assumption that the TCO/a-Si:H(n) contact is a flatband one. The results indicate that $N_e$ is required to be higher than $1\times10^{20}\,cm^{-3}$, preferably higher than $2\times10^{20}\,cm^{-3}$, to obtain a good performance. The requirement for such a high doping concentration is due to the small conduction band offset between a-Si:H and c-Si, as well as the distribution of the gap states in a-Si:H and the interface states of a-Si:H/c-Si. Such defect states have a pinning effect to limit the movement of Fermi level ($E_f$) in the a-Si:H(n) emitter. When $N_e$ is $2\times10^{20}\,cm^{-3}$, AFORS-HET shows $E_f$ of the a-Si:H(n) emitter is already only 0.04 eV away from the edge of the conduction band. This means

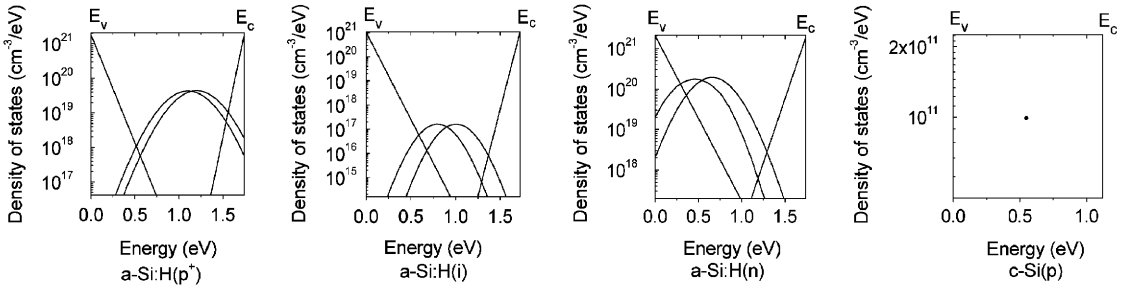


Fig. 1. The gap state distribution of different types of a-Si:H layers and c-Si(p) in the simulations.

Table 1
Some initial parameter values adopted for the bifacial HIT solar cells in the simulations

| Parameters | a-Si:H ($p^+$) | a-Si:H (i) | a-Si:H (n) | c-Si (p) |
|---|---|---|---|---|
| Layer thickness (nm) | 10 | 3 | 10 | $3\times10^{5}$ |
| Dielectric constant | 11.9 | 11.9 | 11.9 | 11.9 |
| Electron affinity (eV) | 3.9 | 3.9 | 3.9 | 4.05 |
| Band gap (eV) | 1.74 | 1.72 | 1.74 | 1.12 |
| Optical band gap (eV) | 1.74 | 1.72 | 1.74 | 1.12 |
| Effective conduction band density ($cm^{-3}$) | $1\times10^{20}$ | $1\times10^{20}$ | $1\times10^{20}$ | $2.8\times10^{19}$ |
| Effective valence band density ($cm^{-3}$) | $1\times10^{20}$ | $1\times10^{20}$ | $1\times10^{20}$ | $1.04\times10^{19}$ |
| Electron mobility ($cm^2\,V^{-1}\,s^{-1}$) | 5 | 5 | 5 | 1040 |
| Hole mobility ($cm^2\,V^{-1}\,s^{-1}$) | 1 | 1 | 1 | 412 |
| Doping concentration of acceptors ($cm^{-3}$) | $1\times10^{20}$ | 0 | 0 | $1\times10^{16}$ |
| Doping concentration of donators ($cm^{-3}$) | 0 | 0 | $1\times10^{20}$ | 0 |
| Thermal velocity of electrons ($cm\,s^{-3}$) | $1\times10^{7}$ | $1\times10^{7}$ | $1\times10^{7}$ | $1\times10^{7}$ |
| Thermal velocity of hole ($cm\,s^{-1}$) | $1\times10^{7}$ | $1\times10^{7}$ | $1\times10^{7}$ | $1\times10^{7}$ |
| Layer density ($g\,cm^{-3}$) | 2.328 | 2.328 | 2.328 | 2.328 |
| Auger recombination coefficient for electron ($cm^6\,s^{-1}$) | 0 | 0 | 0 | 0 |
| Auger recombination coefficient for hole ($cm^6\,s^{-1}$) | 0 | 0 | 0 | 0 |
| Direct band-to-band recombination coefficient ($cm^3\,s^{-1}$) | 0 | 0 | 0 | 0 |

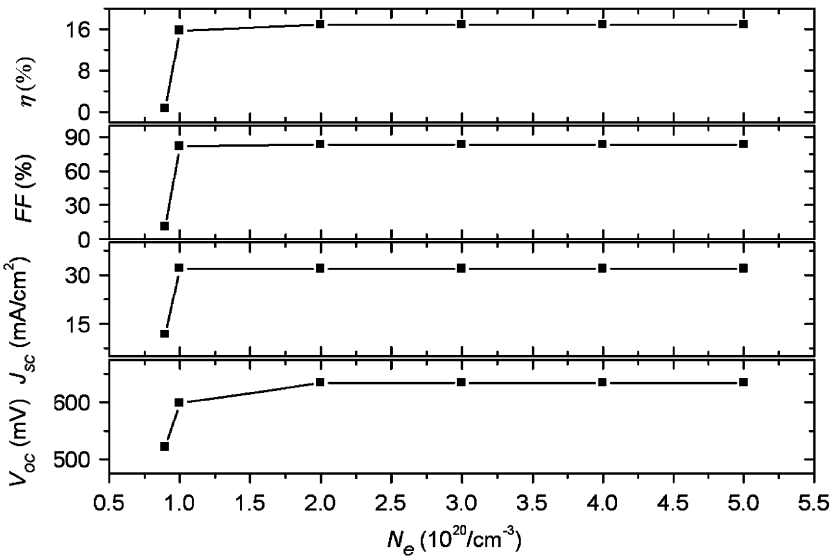


Fig. 2. The simulated performance of the TCO/a-Si:H(n)/c-Si(p) solar cell as a function of the a-Si:H(n) doping concentration ($N_e$) with the TCO/a-Si:H(n) contact as a flatband one, where $\eta$ is the efficiency, FF the fill factor, $J_{SC}$ the short-circuit current density, and $V_{OC}$ the open-circuit voltage.

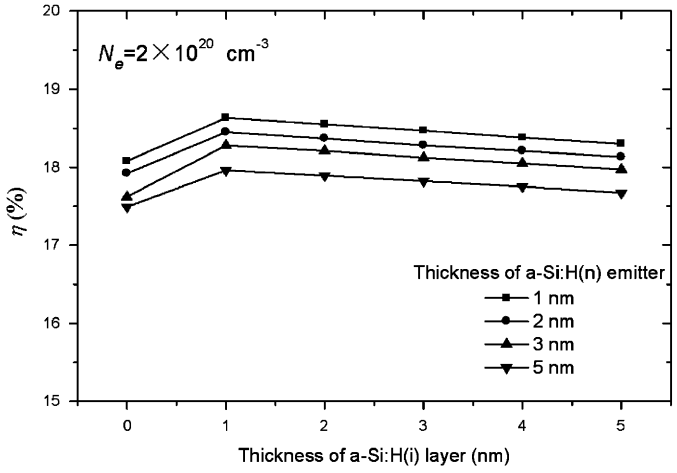


Fig. 3. The simulated efficiency of the TCO/a-Si:H(n)/a-Si:H(i)/c-Si(p) solar cell versus the thickness of the inserted a-Si:H(i) layer with the TCO/a-Si:H(n) contact as a flatband one, where the a-Si:H(n) doping concentration ($N_e$) is $2\times10^{20}\,cm^{-3}$.

the activation energy of electrons is 0.04 eV, which is too low and can hardly decrease further even if $N_e$ becomes much higher. So, when $N_e$ is up to $2\times10^{20}\,cm^{-3}$, the solar cell performance is almost unchanged as $N_e$ increases, which can be obviously seen in Fig. 2. Furthermore, a very high $N_e$ is unacceptable because of the inferior optoelectronic properties of the heavy doped a-Si:H emitter. Hence, it can be considered that $N_e$ of $2\times10^{20}\,cm^{-3}$ can be essentially representative of the acceptable high doping concentration.

### 3.1.2. Influence of the intrinsic a-Si:H layer thickness

In order to passivate the amorphous/crystalline interface, an a-Si:H(i) layer is inserted between the emitter and the base to construct the HIT structure. The a-Si:H(i) layer insertion also has another advantage. Since the diffusion length of free carriers is short in the a-Si:H layer, the carrier transport has a higher efficiency by electric field drift than by diffusion. The thin a-Si:H(i) layer insertion can enhance the width of the depletion region in the two a-Si:H layers to increase the contribution of the drift current at the cost of a little decreased electric field strength. Fig. 3 gives the simulated efficiency ($\eta$) of the TCO/a-Si:H(n)/a-Si:H(i)/c-Si(p) solar cell versus the thickness of the inserted a-Si:H(i) layer with the TCO/a-Si:H(n) contact as a flatband one and $N_e = 2\times10^{20}\,cm^{-3}$. Although the best efficiency is obtained with 1 nm a-Si:H(i) layer insertion, the solar cell efficiency only decreases slightly while the a-Si:H(i) layer thickness increases, but is not over 5 nm. So 3 nm a-Si:H(i) thickness is preferred in accordance with the actual fabrication process [10].

### 3.1.3. Influence of the front TCO/a-Si:H(n) contact

Fig. 4 shows the dependence of the TCO/a-Si:H(n)/a-Si:H(i)/c-Si(p) solar cell performance on the emitter thickness with the variation of $W_{TCO}$ and $N_e$. The inserted a-Si:H(i) layer is 3 nm. It can be seen obviously that along with the increase of the emitter thickness, the solar cell efficiency will increase firstly and then decrease gradually. There is an optimized thickness ($w_{th}$) of the emitter to obtain the best solar cell efficiency. As $W_{TCO}$ lowers and/or $N_e$ increases, $w_{th}$ will decrease.

To understand this, it needs to take into account the energy band alignment of such solar cell, as typically depicted in Fig. 5. The TCO/a-Si:H(n) Schottky contact and the a-Si:H(n)/c-Si(p) junction locate on each side of the emitter, respectively. When $W_{TCO}$ is low, $E_f$ of TCO is higher than that of a-Si:H(n) and thus the built-in potential ($V_D$) of the TCO/a-Si:H(n) Schottky contact has the same direction to that of the a-Si:H(n)/c-Si(p) junction, as shown in the lower part of Fig. 5. However, while $W_{TCO}$ is high, $V_D$ of the TCO/a-Si:H(n) Schottky contact will have an

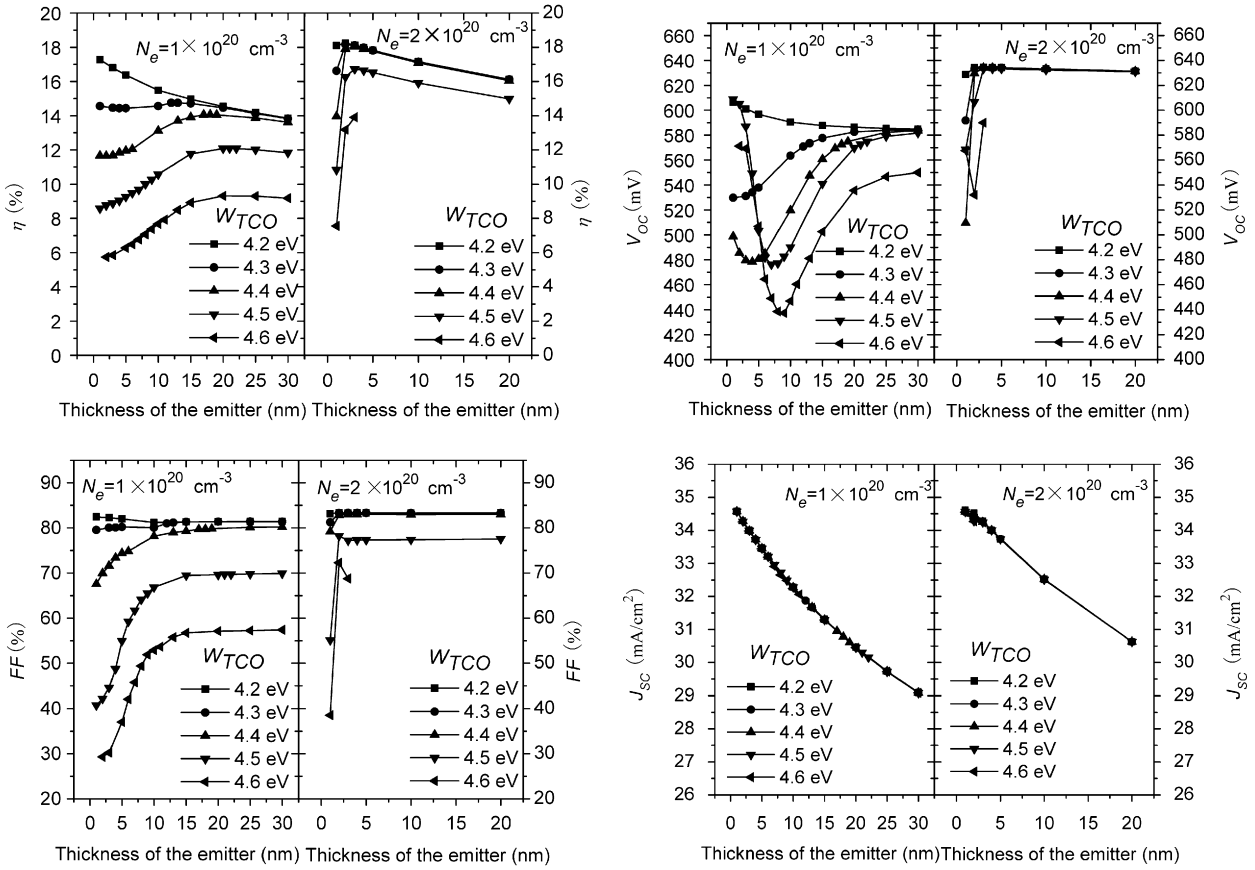


Fig. 4. The simulated performance of the TCO/a-Si:H(n)/a-Si:H(i)/c-Si(p) solar cell as a function of the emitter thickness with various $W_{TCO}$ and $N_e$, where, the inserted a-Si:H(i) layer is 3 nm. $\eta$ is the efficiency, FF the fill factor, $J_{SC}$ the short-circuit current density, and $V_{OC}$ the open-circuit voltage.

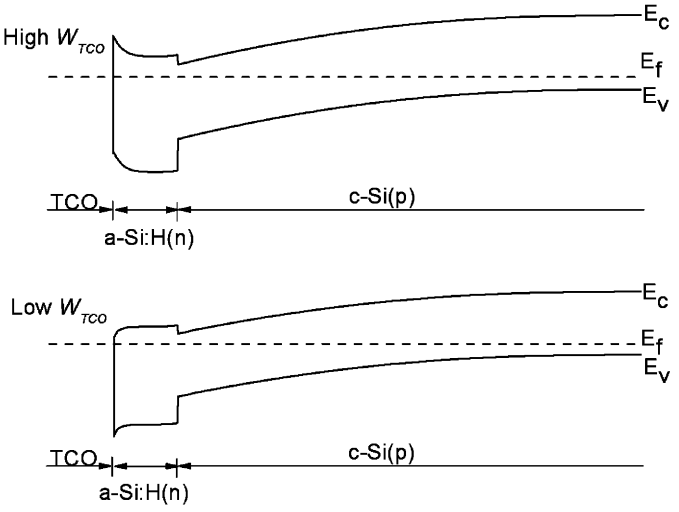


Fig. 5. The diagrammatic energy band alignment of the TCO/a-Si:H(n)/a-Si:H(i)/c-Si(p) structure with a low or a high $W_{TCO}$. The very thin a-Si:H(i) layer is not labelled out. $E_c$ is the edge of conduction band, $E_f$ the Fermi level, and $E_v$ the edge of the valence band.

inverted direction to that of the a-Si:H(n)/c-Si(p) junction, as shown in the upper part of Fig. 5. With the increase of $W_{TCO}$, $V_D$ of the TCO/a-Si:H(n) Schottky contact increases and the corresponding depletion region in the emitter widens, eventually resulting in the overlapping between the TCO/a-Si:H(n) contact region and the a-Si:H(n)/c-Si(p) junction region if the emitter is not thick enough. Thus, the inverted TCO/a-Si:H(n) contact will reduce $V_D$ of the a-Si:H(n)/c-Si(p) junction. In turn, $V_{OC}$ and the fill factor (FF) of the solar cell will decrease.

Although it can be found in Fig. 4 that $V_{OC}$ increases contrarily in some case with a high $W_{TCO}$ and a low emitter thickness, this appearance is not contradictory to the above discussion. It can be clearly understood with the solar cell $J$–$V$ curves shown in Fig. 6. Herein, the TCO/a-Si:H(n) Schottky contact has become the dominant one, and the a-Si:H(n)/c-Si(p) contact has a little effect, or even only plays an inserted layer role in the TCO/c-Si(p) structure. This makes the solar cell $J$–$V$ curve present an obvious S-shape. The severer such an effect is, the lower the inflection voltage will be. As a result, once the inflection occurs ahead of $V_{OC}$, $V_{OC}$ will increase, but FF will decrease greatly. The solar cell obtained by this has a very inferior performance and is unacceptable.

Hence, the thickness of the emitter should be equal to or a little larger than the width sum of the depletion regions of the TCO/a-Si:H(n) contact and the a-Si:H(n)/c-Si(p) junction inside the emitter. Otherwise, the thick emitter will be an optical dead layer for the solar cell due to its inferior properties compared with c-Si. Such an optical dead layer effect will result in the decreased short-circuit

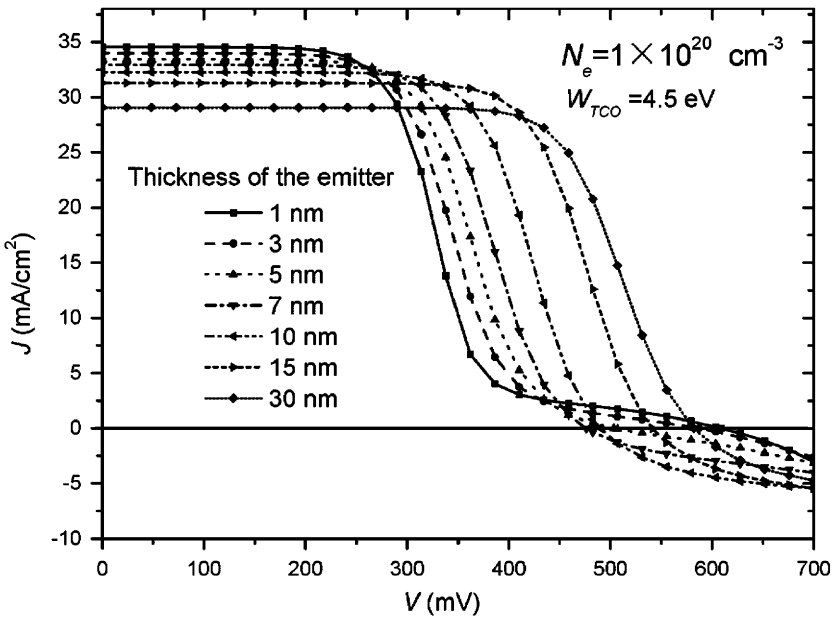


Fig. 6. $J$–$V$ curve of the TCO/a-Si:H(n)/a-Si:H(i)/c-Si(p) solar cell versus the thickness of the emitter, where $N_e = 1 \times 10^{20}\,cm^{-3}$ and $W_{TCO} = 4.5\,eV$. $J$ is the current density and $V$ the applied voltage.

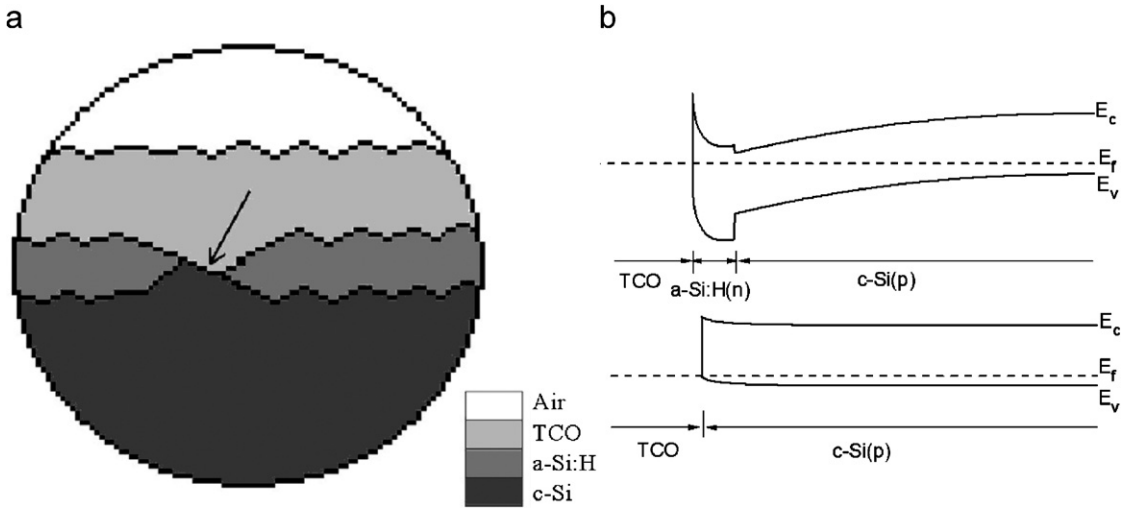


Fig. 7. (a) The possible architecture of the TCO/a-Si:H(n)/a-Si:H(i)/c-Si(p) solar cell with the direct TCO/c-Si(p) contact in practice (the layer thickness is not to scale). (b) The comparative energy band alignments of the TCO/a-Si:H(n)/a-Si:H(i)/c-Si(p) and the TCO/c-Si(p) structures with a high $W_{TCO}$, where the very thin a-Si:H(i) layer is not labelled out.

current density ($J_{SC}$). So the thickness of the emitter should also be not too large. Accordingly, it can be deduced that for any given $W_{TCO}$ and $N_e$, there is a minimal thickness of the emitter to obtain the optimized solar cell performance based on the compromise between the above two effects. Such an appropriate thickness of the emitter is just the above $w_{th}$.

The depicted results of Fig. 4 show that the best performance for the TCO/a-Si:H(n)/a-Si:H(i)/c-Si(p) solar cell can only be obtained under the following conditions: $N_e$ should be equal to or higher than $2 \times 10^{20}\,cm^{-3}$, $W_{TCO}$ should be at least lower than 4.5 eV, and the corresponding $w_{th}$ is about 2 nm. If the obtained $N_e$ can only reach to $1 \times 10^{20}\,cm^{-3}$ or less, both of the solar cell performance and $w_{th}$ will be affected by $W_{TCO}$ greatly. The solar cell efficiency will be much inferior to the highest one and $w_{th}$ has to be several dozen nanometres unless $W_{TCO}$ is low enough.

In fact, $W_{TCO}$ of the conventional TCO, such as indium-tin-oxide (ITO), ZnO and so on, is usually high, generally in the range of 4.5–5.2 eV [16,17]. This will make it difficult to fabricate the TCO/a-Si:H(n)/a-Si:H(i)/c-Si(p) solar cell with a high performance. Furthermore, if the thin a-Si:H layers are deposited nonuniformly in practice, TCO will contact with the c-Si(p) substrate directly in some positions as indicated by the arrow in Fig. 7(a). In this case, if $W_{TCO}$

is so high that $E_f$ of TCO is lower than that of c-Si(p), $V_D$ of the TCO/c-Si(p) contact will also have an inverted direction to that of the a-Si:H(n)/c-Si(p) junction, as shown in Fig. 7(b). The inverted TCO/c-Si(p) Schottky contact will thus induce the short-circuit current channels for the current generating from the a-Si:H(n)/c-Si(p) junction, resulting in the reduction of $J_{sc}$ and $V_{OC}$. $E_f$ of the utilized c-Si(p) substrate here is −4.99 eV. If $W_{TCO}$ is higher than 4.99 eV, the above problem must be considered carefully in the fabrication of the TCO/a-Si:H(n)/c-Si(p) solar cell.

The similar simulation was further carried out for the TCO/a-Si:H(p)/a-Si:H(i)/c-Si(n) solar cell. The results show that although $N_e$ and $W_{TCO}$ are both needed to be high for obtaining a high solar cell performance, $N_e$ of $1\times10^{20}\,cm^{-3}$ and $W_{TCO}$ of 5.1–5.2 eV are enough to meet this requirement. In this case, $w_{th}$ is about 2 nm. Such conditions can be obtained easily in practice. Furthermore, the utilized c-Si(n) base is usually with the resistivity of about 1.0 Ω cm, and its corresponding $E_f$ is about −4.27 eV. The factual $W_{TCO}$ is always higher than 4.27 eV in any case. Thus, even if TCO contacts with the c-Si(n) base directly, just like that occurs in Fig. 7(a), $V_D$ of the TCO/c-Si(n) contact is at most less than that of the a-Si:H(p)/c-Si(n) junction, but they still have the same direction. So the short-circuit current channels like that generate in the HIT solar cell on c-Si(p) do not exist.

Hence, the conventional TCO with a high $W_{TCO}$ is only suitable for the emitter of HIT solar cells on c-Si(n) substrates. An alternative TCO with a low $W_{TCO}$ should be exploited to promote the performance of the HIT solar cells on c-Si(p) substrates. Cesium-incorporated ITO film may be one candidate to meet this requirement. It was found that cesium incorporation could reduce the work function of ITO 0.3–0.4 eV [18].

### 3.2. Optimization of the back structure

#### 3.2.1. Influence of the a-Si:H($p^+$) doping concentration ($N_b$)

Fig. 8 gives the performance of the TCO/a-Si:H(n)/a-Si:H(i)/c-Si(p)/a-Si:H(i)/a-Si:H($p^+$) solar cell as a function of $N_b$ with the assumption that the back contact is a flatband one, where $W_{TCO}$ for the front contact is 4.3 eV, $N_e$ is $2\times10^{20}\,cm^{-3}$, the thickness of the a-Si:H(n) and a-Si:H(i) layers is 2 and 3 nm, respectively. The results indicate that $N_b$ is required to be higher than $1\times10^{20}\,cm^{-3}$ in order to obtain a good performance. Such a high $N_b$ mainly improves FF and $V_{OC}$, and thus the efficiency of the solar cell. As shown in Fig. 9, the conduction band offset

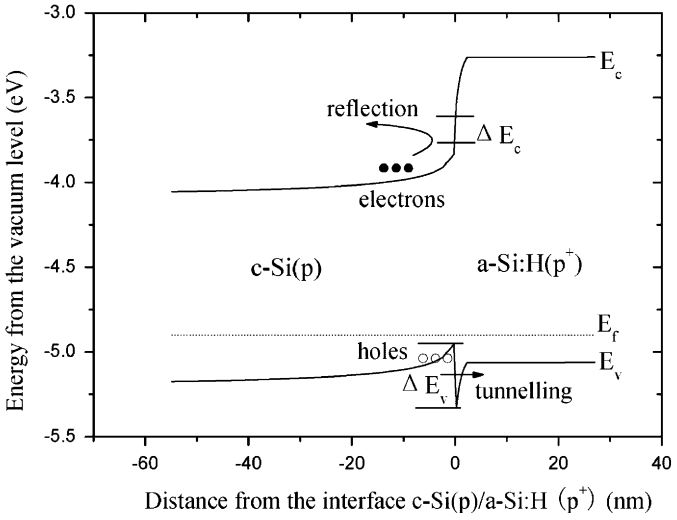


Fig. 9. The mechanism of the a-Si:H($p^+$) back surface field for HIT solar cells on p-type substrates.

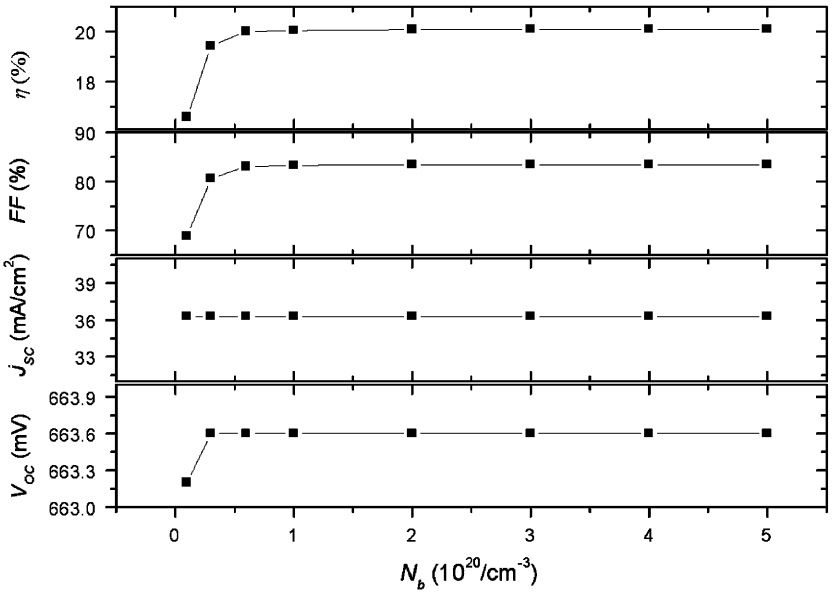


Fig. 8. The simulated performance of the TCO/a-Si:H(n)/a-Si:H(i)/c-Si(p)/a-Si:H(i)/a-Si:H($p^+$) solar cell versus the doping concentration of the a-Si:H($p^+$) layer ($N_b$) with the back contact as a flatband one, where the optimized front structure is adopted. $\eta$ is the efficiency, FF the fill factor, $J_{SC}$ the short-circuit current density, and $V_{OC}$ the open-circuit voltage.

between a-Si:H and c-Si is about 0.15 eV, the valence band offset is yet about 0.45 eV. The essentially unchanged $J_{SC}$ in Fig. 8 indicates that such a conduction band offset can play a good role to reflect the minority carriers, electrons here. But the large valence band offset makes a barrier for the tunnelling of the majority carriers, holes here. In order to enhance the tunnelling opportunity, a high $N_b$ is needed to reduce the barrier width, and thus to improve FF and $V_{OC}$.

### 3.2.2. *Influence of the back a-Si:H($p^+$)/TCO contact*

Fig. 10 shows the dependence of the TCO/a-Si:H(n)/a-Si:H(i)/c-Si(p)/a-Si:H(i)/a-Si:H($p^+$)/TCO solar cell performance on the a-Si:H($p^+$) BSF thickness with the variation of the back TCO work function ($W_b$), where $N_b$ of $1\times10^{20}\,cm^{-3}$ was further adopted. The results demonstrate that a low $W_b$ can make the solar cell performance inferior. The mechanism is the same as the former described for the front contact. A thick a-Si:H($p^+$) layer can overcome the negative effect of the back a-Si:H($p^+$)/TCO contact. For example, when $W_b$ is 5.2 eV, 5 nm a-Si:H($p^+$) layer is needed to obtain the best solar cell performance. A thicker a-Si:H($p^+$) layer will not lead to the performance decrease, because the sunlight is supposed to illuminate on the front surface only and thus no optical dead layer effect occurs for the a-Si:H($p^+$) layer. So, if the solar cell is not for the bifacial application, the a-Si:H($p^+$) layer can have a relative large thickness in accordance with some process requirements as long as it is conductive enough.

Furthermore, when $W_b$ is higher than 5.6 eV, Fermi level of TCO will be lower than the edge of the valence band of the a-Si:H($p^+$) layer. As a result, $V_D$ of the c-Si(p)/TCO Schottky contact is essentially higher than that of the c-Si(p)/a-Si:H($p^+$) junction. The c-Si(p)/TCO contact may have a better BSF effect than the c-Si(p)/a-Si:H($p^+$) junction does. Hence, it is possible to omit the a-Si:H($p^+$) layer. However, in this case, for the factual solar cell, the interface quality of the c-Si(p)/TCO contact will become another crucial factor, which should be considered carefully.

In the above simulations, the light reflection of the front and the back contacts was set to be 0.1 and 1, respectively. For the real solar cell, such reflection can be controlled by adjusting the thickness of TCO and/or adopting some texture structures on the surfaces. The front reflection

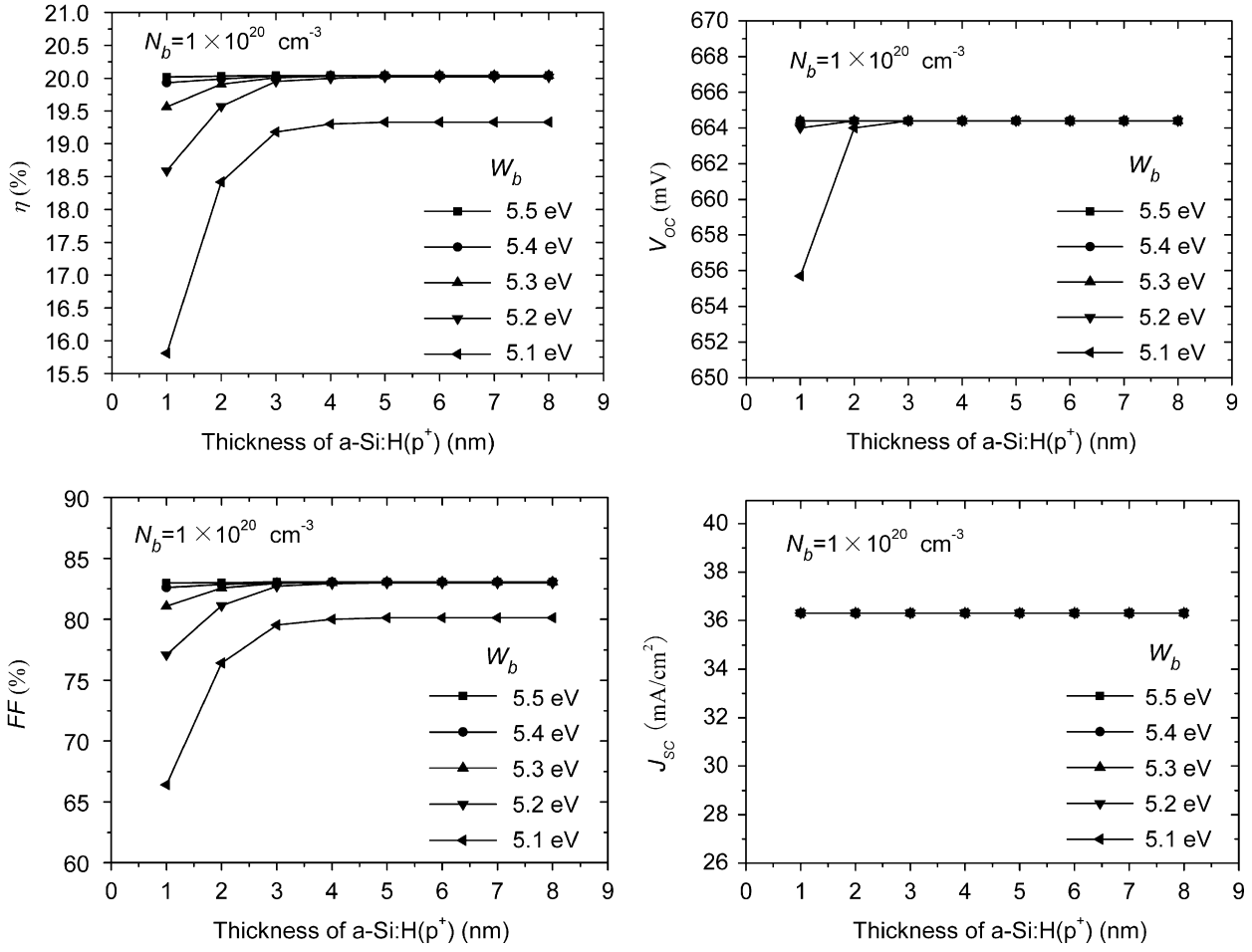


Fig. 10. The simulated performance of the TCO/a-Si:H(n)/a-Si:H(i)/c-Si(p)/a-Si:H(i)/a-Si:H($p^+$)/TCO solar cell as a function of the a-Si:H($p^+$) BSF thickness with various work function of the back TCO contact ($W_b$), where $N_b = 1\times10^{20}\,cm^{-3}$ and the optimized front structure is adopted. $\eta$ is the efficiency, FF the fill factor, $J_{SC}$ the short-circuit current density, and $V_{OC}$ the open-circuit voltage.

Table 2
The optimized parameters for the bifacial HIT solar cells on p-type substrates

| Layer | Thickness (nm) | The doping concentration ($cm^{-3}$) | Work function (eV) |
|---|---|---|---|
| Front TCO | 80 | – | $<4.5$ |
| a-Si:H(n) | ~2 | $2\times10^{20}$ or above | – |
| a-Si:H(i) | 3 | – | – |
| c-Si(p) | 300 | $1\times10^{16}$ | – |
| a-Si:H(i) | 3 | – | – |
| a-Si:H($p^+$) | ~5 | $1\times10^{20}$ or above | – |
| Back TCO | 80 | – | $>5.2$ |

should be as low as possible, especially for the visible light. And the back internal reflection should be high instead, especially for the light with longer wavelength. In the previous research, the thickness of TCO has been optimized to be 80 nm for obtaining the lowest reflectance at the wavelength of about 600 nm [3,8]. For the bifacial application, such TCO thickness can be utilized for both the front and the back surfaces. If the single-sided application is considered, a high reflectance metal layer can be deposited further on the back TCO.

In summary, the design optimization of the bifacial HIT solar cells on the c-Si(p) substrates was provided. All the optimized parameters are generalized in Table 2. Based on this, the HIT solar cells with the higher performance can be achieved on the c-Si(p) substrates by further improving the quality of all the material layers and all the interfaces.

## 4. Conclusions

The performance of the TCO/a-Si:H(n)/a-Si:H(i)/c-Si(p)/a-Si:H(i)/a-Si:H($p^+$)/TCO solar cell was investigated in detail by utilizing AFORS-HET software as a numerical simulation tool. The influence of various parameters for the front and the back structures was studied. And the corresponding design optimization was provided.

The work function of transparent conductive oxide ($W_{TCO}$) can affect the HIT performance obviously. If $W_{TCO}$ is not appropriate, the built-in potentials ($V_D$) of the TCO/a-Si:H contact and the a-Si:H/c-Si junction will have the opposite directions to each other. In this case, the depletion region overlapping between the two junctions will result in the decrease of the solar cell performance. Hence, the thickness of the a-Si:H layer should be equal to or a little larger than the width sum of the depletion regions of the above two junctions inside the said a-Si:H layer. Further, there is an optimized thickness ($w_{th}$) of the emitter to obtain the best solar cell efficiency while the optical dead layer effect of the a-Si:H layer is further involved.

For the front TCO/a-Si:H(n)/a-Si:H(i)/c-Si(p) structure, $W_{TCO}$ should be as low as possible. In order to obtain the high solar cell performance, the doping concentration of the a-Si:H(n) emitter ($N_e$) should be equal to or higher than $2\times10^{20}\,cm^{-3}$, $W_{TCO}$ should be at least lower than 4.5 eV and the corresponding $w_{th}$ is about 2 nm. A 3 nm a-Si:H(i) layer is preferred to passivate the amorphous/crystalline interface.

For the back c-Si(p)/a-Si:H(i)/a-Si:H($p^+$)/TCO structure, 3 nm a-Si:H(i) layer is also preferred. The work function of the back TCO ($W_b$) should be as high as possible. The optimized conditions are $W_b$ is 5.2 eV or above, the doping concentration of the a-Si:H($p^+$) layer ($N_b$) is equal to or higher than $1\times10^{20}\,cm^{-3}$, and the thickness of a-Si:H($p^+$) layer is about 5 nm. A thicker a-Si:H($p^+$) layer can be adopted to meet some process requirements as long as it is conductive enough. And if $W_b$ is especially high, it is possible to omit the a-Si:H($p^+$) layer. The c-Si(p)/TCO Schottky contact can be utilized as the BSF directly, but the c-Si(p)/TCO interface should be controlled perfectly.

## Acknowledgement

This work was supported by the 863 high technology research program of China (Grant no. 2006AA05Z405).

## References

[1] T. Sawada, N. Terada, S. Tsuge, T. Baba, T. Takahama, K. Wakisaka, S. Tsuda, S. Nakano, High-efficiency a-Si:H/c-Si heterojunction solar cells, in: Proceedings of the First WCPEC Conference, Hawaii, USA, 1994, pp. 1219–1226.
[2] C. Voz, D. Muñoz, M. Fonrodona, I. Martin, J. Puigdollers, R. Alcubilla, J. Escarre, J. Bertomeu, J. Andreu, Bifacial heterojunction silicon solar cells by hot-wire CVD with open-circuit voltages exceeding 600 mV, Thin Solid Films 511–512 (2006) 415.
[3] M. Tucci, M. della Noce, E. Bobeico, F. Roca, G. de Cesare, F. Palma, Comparison of amorphous/crystalline heterojunction solar cells based on n- and p-type crystalline silicon, Thin Solid Films 451–452 (2004) 355.
[4] Y. Xu, Z.H. Hu, H.W. Diao, Y. Cai, S.B. Zhang, X.B. Zeng, H.Y. Hao, X.B. Liao, E. Fortunato, R. Martins, Heterojunction solar cells with n-type nanocrystalline silicon emitters on p-type c-Si wafers, J. Non-Cryst. Solids 352 (2006) 1972.
[5] P.J. Rostan, U. Rau, V.X. Nguyen, T. Kirchartz, M.B. Schubert, J.H. Werner, Low-temperature a-Si:H/ZnO/Al back contacts for high-efficiency silicon solar cells, Sol. Energy Mater. Sol. Cells 90 (2006) 1345.
[6] H.D. Goldbach, A. Bink, R.E.I. Schropp, Thin $p^{++}$ μc-Si layers for use as back surface field in p-type silicon heterojunction solar cells, J. Non-Cryst. Solids 352 (2006) 1872.
[7] Y. Veschetti, J.C. Muller, J.R. Damon-Lacoste Cabarrocas, A.S. Gudovskikh, J.P. Kleider, P.J. Ribeyron, E. Rolland, Optimisation of amorphous and polymorphous thin silicon layers for the formation of the front-side of heterojunction solar cells on p-type crystalline silicon substrates, Thin Solid Films 511–512 (2006) 543.
[8] K.v. Maydell, E. Conrad, M. Schmidt, Efficient silicon heterojunction solar cells based on p- and n-type substrates processed at temperatures $<220\,^{\circ}C$, Prog. Photovolt. Res. Appl. 14 (2006) 289.
[9] Stefaan Wolf De, Beaucarne Guy, Surface passivation properties of boron-doped plasma-enhanced chemical vapor deposited hydrogenated amorphous silicon films on p-type crystalline Si substrates, Appl. Phys. Lett. 88 (2006) 022104.
[10] Q. Wang, M.R. Page, E. Iwaniczko, Y.Q. Xu, L. Roybal, R. Bauer, D. Levi, Y.F. Yan, D. Meier, T.H. Wang, H.M. Branz, Silicon hetero junction solar cells by hot-wire CVD, in: ISES Solar World Congress, Beijing, China, 2007, pp. 1144–1147.

[11] R. Stangl, A. Froitzheim, M. Schmidt, W. Fuhs, Design criteria for amorphous/crystalline silicon heterojunction solar cells—a simulation study, in: Proceedings of the Third World Conference on Photovoltaic Energy Conversion, Osaka, Japan, 2003, pp. 1005–1008.
[12] A. Froitzheim, R. Stangl, L. Elstner, M. Schmidt, W. Fuhs, Interface recombination in amorphous/crystalline silicon solar cell, a simulation study, in: Conference Record of the 29th IEEE Photovoltaic Specialists Conference, New Orleans, USA, 2002, pp. 1238–1241.
[13] Z.H. Hu, X.B. Liao, X.B. Zeng, Y.Y. Xu, S.B. Zhang, H.W. Diao, G.L. Kong, Computer simulation of a-Si:H/c-Si heterojunction solar cells, Acta Phys. Sin. 52 (2003) 217.
[14] Centurioni Emanuele and Iencinella Daniele, Role of front contact work function on amorphous silicon/crystalline silicon heterojunction solar cell performance, IEEE Electron Dev. Lett. 24 (2003) 177.
[15] M. Schmidt, L. Korte, A. Laades, R. Stangl, Ch. Schubert, H. Angermann, E. Conrad, K.V. Maydell, Physical aspects of a-Si:H/c-Si heterojunction solar cells, Thin Solid Films 515 (2007) 7475.
[16] T. Minami, T. Miyata, T. Yamamoto, Work function of transparent conducting multicomponent oxide thin films prepared by magnetron sputtering, Surf. Coat. Technol. 108–109 (1998) 583.
[17] J.S. Kim, B. Lägel, E. Moons, N. Johansson, I. Baikie, W.R. Salaneck, R.H. Friend, F. Cacialli, Kelvin probe and ultraviolet photoemission measurements of indium tin oxide work function: a comparison, Synth. Met. 111–112 (2000) 311.
[18] T. Uchida, T. Mimura, M. Ohtsuka, T. Otomo, M. Ide, A. Shida, Y. Sawada, Cesium-incorporated indium-tin-oxide films for use as a cathode with low work function for a transparent organic light-emitting device, Thin Solid Films 496 (2006) 75.